Stereochemically Controlled Gel

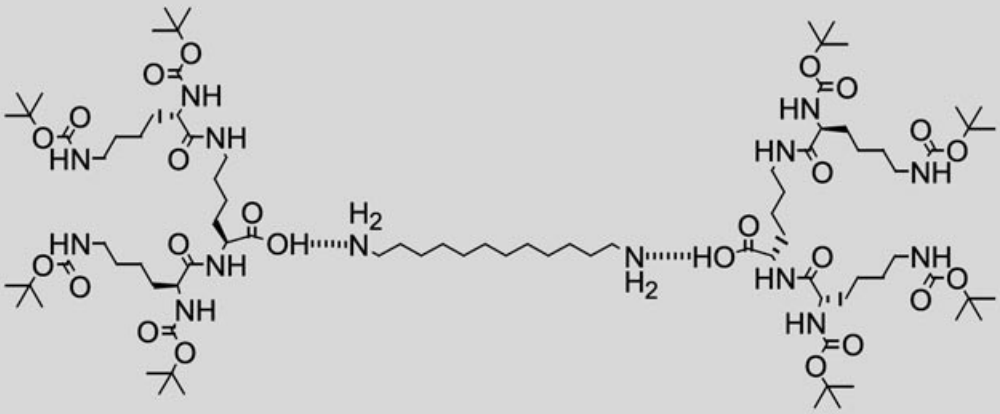

The chirality of the dendritic peptides controls the self-assembly into fibres

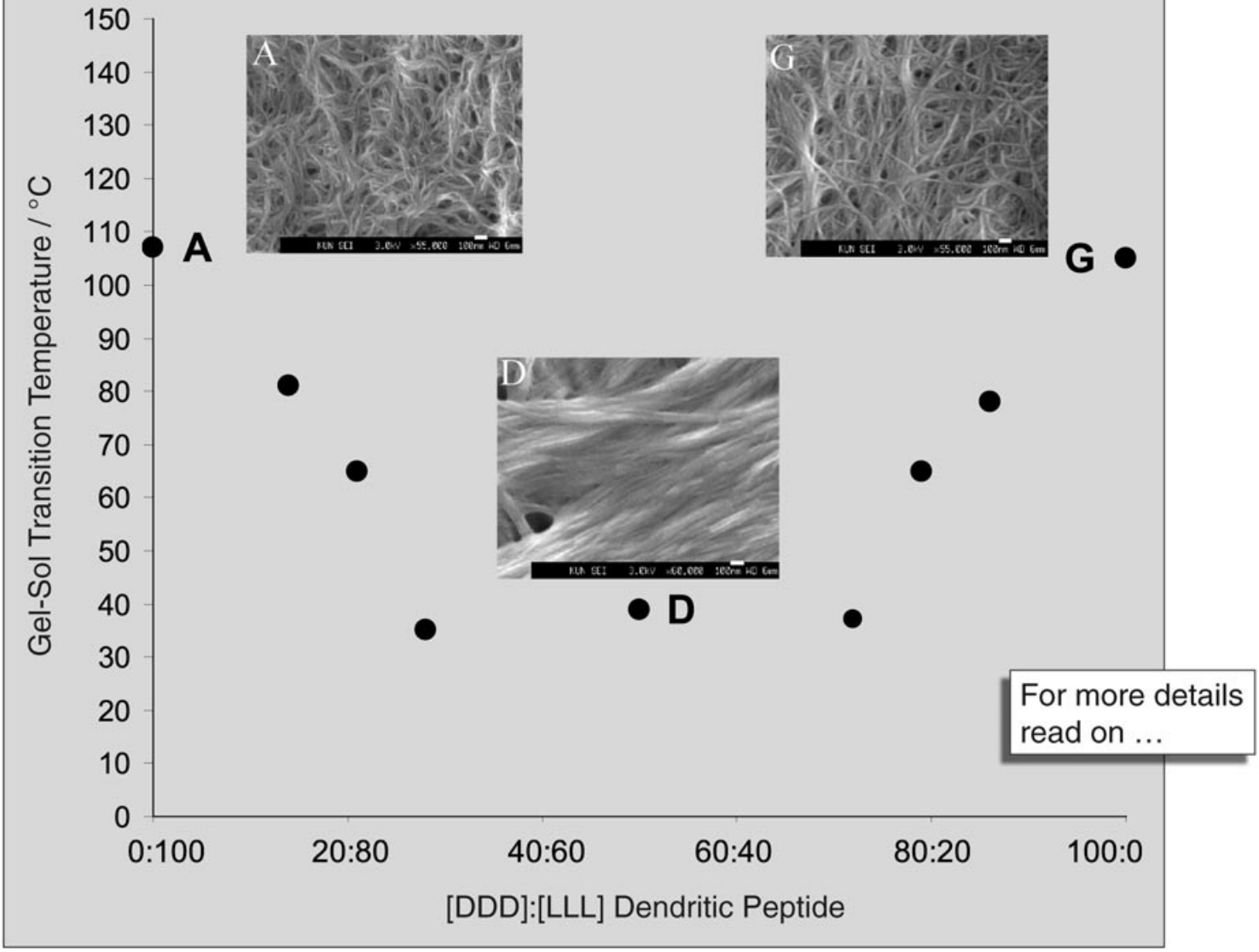

 DOI: 10.1002/chem.200400502

VIP

Two-Component Dendritic Gel: Effect of Stereochemistry on the Supramolecular Chiral Assembly

Andrew R. Hirst,[a] David K. Smith,*[a] Martin C. Feiters,[b] and Huub P. M. Geurts[c]

Abstract: The self-assembly of diaminododecane solubilised by four different stereoisomeric dendritic peptides to form gel-phase materials in toluene was investigated. The second generation dendritic peptides were based on D- and L-lysine building blocks, and each contained three chiral centres. By designing dendritic peptides in which the configurations of the chiral centres were modified, and applying them as gelator units, the assembly of stereoisomers could be investigated. In all cases, the self-assembly of gelator units resulted in macroscopic gelation. However, the degree of structuring was modulated by the stereoisomers employed, an effect which changed the morphology and macroscopic behavior of the self-assembled state. Enantiomeric (L,L,L or D,D,D) gelator units formed fibrous molecular assemblies, whilst the racemic gel (50% L,L,L : 50% D,D,D) formed a flat structure with a "woven" appearance. Gelator units based on L,D,D or D,L,L dendritic peptides also formed fibrous assemblies, but small-angle X-ray scattering indicated significant morphological differences were caused by the switch in chirality. Furthermore, the macroscopic stability of the gel was diminished when these peptides were compared with their L,L,L or D,D,D analogues. In this paper it is clearly shown that individual stereocentres, on the molecular level, are directly related to the helicity within the fibre. It is argued that the chirality controls the pattern of hydrogen bonding within the assembly, and hence determines the extent of fibre formation and the macroscopic gel strength.

Keywords: chirality · dendrimers · gels · nanotechnology · supramolecular chemistry

Introduction

The self-assembly of molecules into helical and multiple helical architectures is a dominant motif in biology and materials science,[1] with the relationship between the microscopic chirality of the self-assembled state and the intrinsic chirality of a molecule or "building block" being a fascinating area of current investigation. The prerequisite for self-assembly is the compatibility of "molecular building blocks" guided by highly directional noncovalent interactions (e.g. hydrogen bonds, π–π stacking, electrostatic interactions, and solvophobic interactions).[2] Molecular or "bottom up" fabrication, using simple building blocks to fashion functional nanoscale assemblies in this way, has been exploited in the emerging fields of biomolecular materials,[3] optoelectronics,[4] and the synthesis of organogels[5] and hydrogels.[6]

The impact of chirality on assembled systems can be profound.[7] Chirality plays key roles in assembly processes taking place on two-dimensional surfaces,[8] in liquid-crystalline phases[9] and, of particular relevance to the work described herein, in the formation of supramolecular polymers[10] and gel-phase materials.[11] In supramolecular organogels, the chirality within an individual molecule or "building block" can be transcribed to the nano- and mesoscale fibrous assemblies. However, the factors responsible for the transmission of chiral information during self-assembly are not fully understood.

It is worthy of note that assembled fibrous structures are of considerable biological significance.[12] The self-assembly of peptidic units is of key importance in the pathways of protein folding diseases,[13] for example amyloidosis[14] and in Creutzfeld-Jacob's disease (CJD).[15] In amyloidosis, point mutation causes proteins to stack together, minimising their exposed hydrophobic surface and packing together β-sheet regions to maximise hydrogen bonding within a fibrillar structure. Initially, small soluble protein assemblies are generated, which later assemble into larger insoluble aggregates, which are a diagnostic symptom of disease.[16] Investigations of the effects of molecular-scale modifications on the nano-,

[a] Dr. A. R. Hirst, Dr. D. K. Smith
University of York
Heslington, York, YO10 5DD (UK)
Fax: (+44) 190-443-2516
E-mail: dks3@york.ac.uk

[b] Dr. M. C. Feiters
University of Nijmegen, NSRIM
Toernooiveld, 6525 ED Nijmegen (Netherlands)

[c] H. P. M. Geurts
Instrumentation, University of Nijmegen
1 Toernooiveld, 6525 ED Nijmegen (Netherlands)

DOI: 10.1002/chem.200400502

micro- and macroscale properties of synthetic fibres is therefore of biomimetic interest.

We have developed a two-component gelation system which uses a dendritic building block based on the amino acid L-lysine in combination with an aliphatic diamine (Scheme 1).[17] We have reported that the molar ratio of the two components plays a key role in controlling the morphology of the gel-phase material. Furthermore, the properties of the gel can be modulated by tuning the core aliphatic spacer unit. We have shown that dendron–dendron hydrogen bonding interactions are largely responsible for the formation of fibrous assemblies. Herein we investigate for the first time the transcription of the stereochemistry of the individual dendritic building blocks. We focus on the gelation behaviour of diaminododecane, solubilised by second generation dendritic peptides based on L and D-lysine and containing three chiral centres (L,L,L and D,D,D). Furthermore, L,D,D and D,L,L peptides in which one chiral centre has been 'switched' have also been studied. The chirality of dendritic molecules has been of considerable interest,[18] and herein we provide an interesting example of ways in which this chirality can be expressed on a microscopic and macroscopic scale in a controlled way.

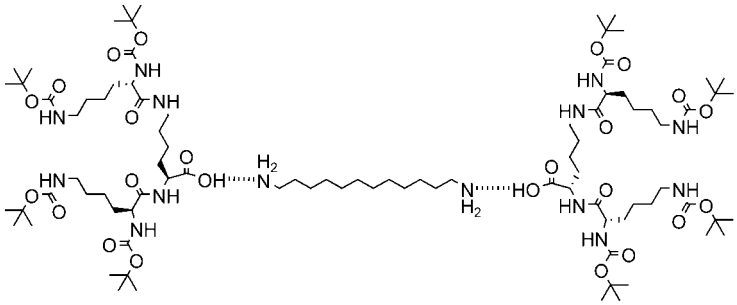

Scheme 1. Structure of dendritic two-component gelator unit.[17]

Results and Discussion

Synthesis: The building block, or gelator unit, that self-assembles, inducing macroscopic gelation of aprotic organic solvents is shown in Scheme 1. Four stereoisomeric dendritic peptides (Scheme 2) were synthesised by using a directly analogous method to that previously reported for L,L,L dendritic lysine (Scheme 3),[19] only replacing the L-lysine with D-lysine at the appropriate points in the synthesis. Our previous studies have unambiguously proven that the stereochemistry of these dendritic peptides is retained when employing this synthetic pathway.[20] Purification was achieved by using silica gel chromatography, and all characterisation data were in full agreement with the assigned structures.

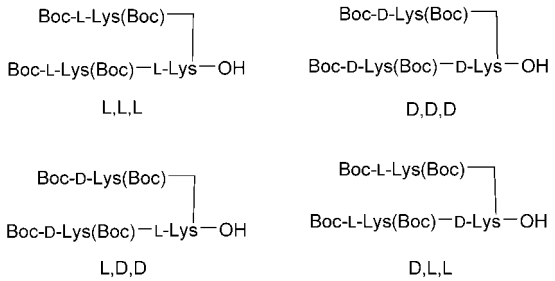

Scheme 2. Schematic structures of the four stereoisomers used in the present study.

Thermal properties of the gel-phase materials: To assess the structuring behavior of the different gelator units, the transition from an immobile to a mobile self-assembled state was determined by using tube-inversion experiments.[21] All the gel-phase materials reported here were generated by using a 2:1 dendritic branch:diaminododecane ratio in toluene, and were thermo-reversible and optically clear, indicating good solubility of the two-component system under all conditions. As previously reported, the effect of molar concentration of the two-component gelator on the T_{gel} (gel–sol transition temperature) may be described in terms of two distinct regions.[17c] Initially, increasing the concentration of the gelator unit increases T_{gel} until eventually a plateau region is reached in which network formation is considered to be complete.

It was found that the gelator stereochemistry profoundly influenced the thermal properties associated with the macroscopic gelation (Figure 1). Both enantiomers have approximately equal gelation properties with respect to the T_{gel} (L,L,L-enantiomer: $T_{gel}=105\,^{\circ}C$; D,D,D-enantiomer: $T_{gel}=107\,^{\circ}C$). This is analogous to the melting points of the enantiomeric solids (see Experimental Section), which are equal because "handedness" does not have an impact on this type

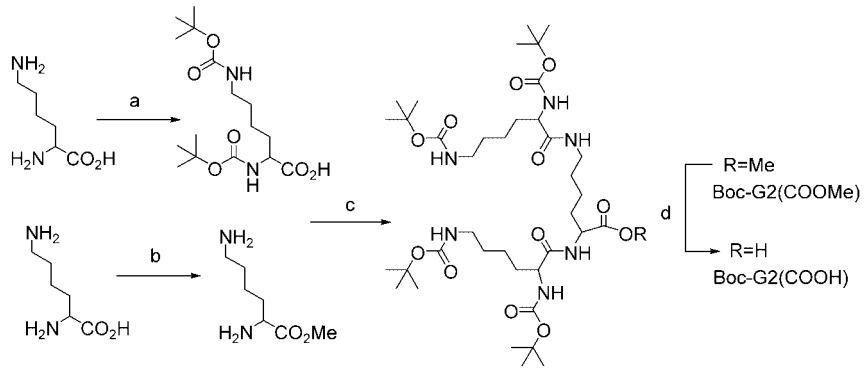

Scheme 3. Synthesis of second generation dendritic peptides (Boc-G2(COOH)).[19,20] a) Boc_2O, NaOH, H_2O, dioxane, 97%; b) 2,2-dimethoxypropane, MeOH, HCl, 93%; c) DCC, HOBt, Et_3N, EtOAc, 82%; d) NaOH, MeOH, H_2O, 90%. DCC = dicyclohexyl carbodiimide, HOBt = 1-hydroxy-1*H*-benzotriazole.

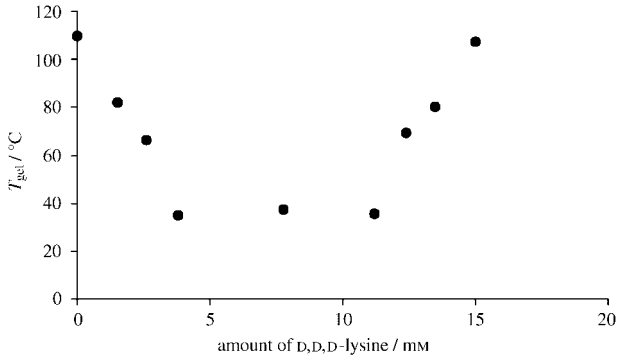

Figure 1. Effect of the amount of D,D,D dendritic peptide on the T_{gel} of the organogel based on the L,L,L dendritic peptide. At each point, [dendritic peptide]$_{total}$ = 15 mM, [$H_2N(CH_2)_{12}NH_2$] = 7.5 mM, solvent = toluene.

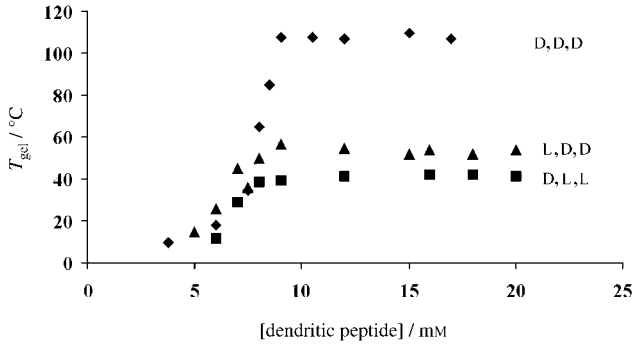

Figure 2. Effect of molar concentration on T_{gel} as a function of the stereochemical configuration of the dendritic peptide. Solvent: toluene.

of phase-transition. Interestingly, when gel-phase materials were generated by using mixtures of the L,L,L and D,D,D dendritic peptides, the degree of macroscopic gelation was significantly reduced. Minimum T_{gel} values were observed when using mixtures in a range between 75:25 and 25:75 (L,L,L:D,D,D), with T_{gel} = 35–40 °C. This implies that introduction of the second enantiomer to the chiral gel network modifies the self-complementary noncovalent interactions and hence the molecular packing of gelator units.[22] The aliphatic diamine was constant in these studies, clearly indicating that the superior gelating properties when using a single enantiomer must be related to the spatial and temporal associative forces which exist between the gelator units.

It has been previously reported that racemates are less efficient gelators than pure enantiomers, and sometimes lack any capacity to gelate because of a propensity to crystallise.[5d,23,24] Additionally, the self-assembly of stereochemically different amphiphilic gelators has been explained in terms of a "chiral bilayer effect". In such cases, racemates are not predisposed to form unidirectional "stacks" or fibres but instead precipitate to form three-dimensional crystal structures.[24] It should therefore be pointed out that crystallisation of the racemic mixture was not observed in this case, and all gels remained optically transparent.

Experiments were also conducted, in which the enantiomeric (L,L,L and D,D,D) dendritic peptides were replaced with their diastereoisomers (L,D,D and D,L,L, Scheme 2). The effect of molar concentration on the thermally reversible "gel boundary", T_{gel} is shown in Figure 2. Switching one chiral centre from the D,D,D peptide to its L,D,D diastereoisomer resulted in a dramatic reduction in the macroscopic gelation behavior (D,D,D: T_{gel} = 107 °C; L,D,D: T_{gel} = 53 °C). As would be expected the behavior of L,D,D and D,L,L dendritic peptides is similar given their enantiomeric relationship. Presumably, the reduction in the macroscopic level of gelation between D,D,D and L,D,D peptides is related to changing the chiral centre, which must lead to disruption of the dendron–dendron hydrogen bonds by modifying the spatial arrangement of gelator units. It is remarkable that changing just a single chiral centre in a relatively complex system can have such a targeted effect. It is often considered that dendritic systems have little long-range conformational order, however, in this case, it is clear that changing the configuration of one chiral centre must significantly perturb the three-dimensional organisation of the dendritic architecture, and that this modification is in turn transcribed up to the nanoscale, mesoscale, and ultimately the macroscopic level. This speculation is proven in the following section describing morphological properties. The precise molecular control of materials properties exhibited by this two-component gelator is reminiscent of the way in which subtle modification of a protein can lead to changes in its folding, hence controlling its preorganisation with respect to the formation of fibrillar aggregates in diseases such as Alzheimer's and CJD.[13]

Morphological properties of the gel-phase materials—scanning electron microscopy (SEM): Molecular self-assembly at the nano- and micro-levels can be observed by using SEM. This technique provides a comparative visual technique to assess the impact of the different dendritic peptide stereoisomers on self-assembly. SEM images (Figure 3a–g) of the organogels formed by using different molar ratios of L,L,L and D,D,D dendritic peptides. The same total concentration of gelator unit was employed in each case. Remarkably, SEM revealed that the morphology of the self-assembled state is directly controlled by the ratio of enantiomers present in the organogel. Organogels assembled from pure L,L,L (Figure 3a) or D,D,D enantiomers (Figure 3g) formed thin fibres that underwent further aggregation to form bundles of fibres. These bundles of fibres constitute a highly developed entangled network. The regular shape and high aspect ratio of the individual fibres indicates uni-directional "stacking" of the gelator units. Analysis of the individual fibres showed that they were approximately 20 nm wide and several hundreds of nanometres long.

Mixing a little of the D,D,D enantiomer with the L,L,L enantiomer also gives rise to a organogel composed of a fibre network (Figure 3b). However, the number and density of fibre bundles drops noticeably, rendering a network composed of a larger number of individual fibres. This subtle change in aggregate morphology is reflected by the decrease in thermal stability of the gel ([L,L,L]:[D,D,D] = 10:0 (mM), T_{gel} = 105 °C; [L,L,L]:[D,D,D] = 8.7:1/3 (mM), T_{gel} = 82 °C). Increasing the mole fraction of the D,D,D-enantiomer even further, produced profound changes in the aggregate morphology (Figure 3c and d). Discrete fibre bundles were replaced

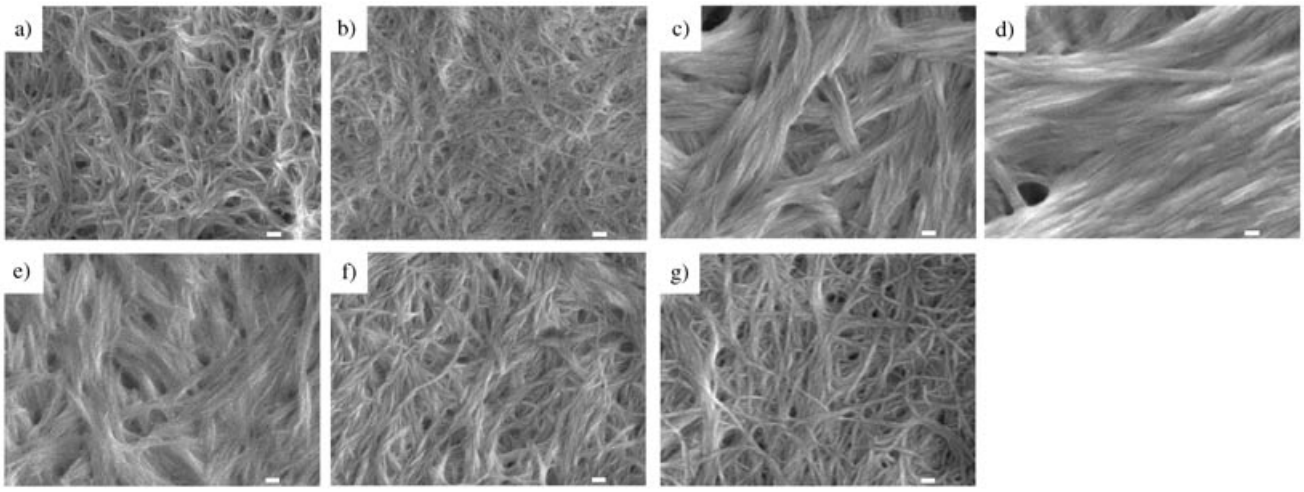

Figure 3. Effect of different molar ratios of L,L,L and D,D,D dendritic peptides on aggregate morphology using SEM. In each case, $[\text{dendritic peptide}]_{total} = 10\,mM$, $[H_2N(CH_2)_{12}NH_2] = 5\,mM$. a) $[L,L,L] = 10\,mM$, $[D,D,D] = 0\,mM$; b) $[L,L,L] = 8.7\,mM$, $[D,D,D] = 1.3\,mM$; c) $[L,L,L] = 6.2\,mM$, $[D,D,D] = 3.8\,mM$; d) $[L,L,L] = 5\,mM$, $[D,D,D] = 5\,mM$; e) $[L,L,L] = 3.8\,mM$, $[D,D,D] = 6.2\,mM$; f) $[L,L,L] = 2.5\,mM$, $[D,D,D] = 7.5\,mM$; g) $[L,L,L] = 0\,mM$, $[D,D,D] = 10\,mM$. The white bar represents a distance of 100 nm.

by large super-structures, which appear to be composed of "ribbon-like" morphologies. Figure 3c indicates that large fibres are formed, which have a diameter of ~400 nm and lengths that are microns long. A 50:50 racemic mixture (Figure 3d) results in a self-assembled state that appears to consist of a small number of inter-woven super-structures in which all fine detail was lost and only extremely large fibres (relative to the micro-scale) were observed. However, it is difficult to determine the approximate dimensions of the "building block" from the SEM image due to the lack of well-defined structures.

Importantly, the stereochemically-driven change in the mode of self-assembly is directly related to the decrease in thermal stability of the gel, which reflects the macroscopic gelation ability, that is, for the L,L,L peptide, $T_{gel} = 105\,°C$ (Figure 3a) while for the racemic mixture of L,L,L and D,D,D peptides, $T_{gel} = 37\,°C$ (Figure 3d). As the mole fraction of the D,D,D enantiomer was increased further, a similar transition in aggregate morphology was observed (Figure 3e and f). This clearly indicates the mirror image relationship of the nanoscale self-assembled aggregates. Once again, these nanostructures are directly related to the mirror-image trends observed in the macroscopic behavior of the gel (Figure 1).

Interestingly, even though the aggregate morphology is dictated by the molar ratio of the two enantiomers, the self-assembly is still predominantly one-dimensional. This would suggest that under the non-polar conditions dictated by the choice of solvent (toluene) there is a strong driving force to maximise the anisotropic nature of the dendron–dendron hydrogen bonds. However, stereochemical effects may influence the packing arrangements or surface curvature of the self-assembled state, hence dictating the observed aggregate morphology.[25]

Intriguingly, subtle differences were also observed when the gels based on L,D,D and D,L,L dendritic lysine were characterised using SEM. Figure 4a and b show the SEM images

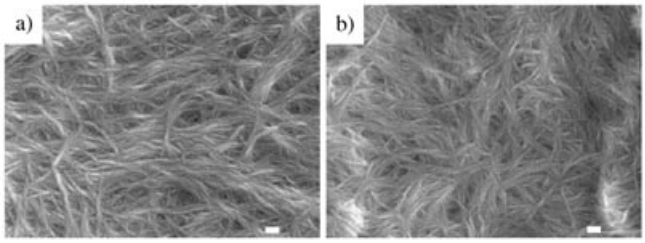

Figure 4. Effect of different diastereoisomers on the aggregate morphology, $[\text{dendritic peptide}]_{total} = 10\,mM$, $[H_2N(CH_2)_{12}NH_2] = 5\,mM$. a) L,D,D dendritic peptide; b) D,L,L dendritic peptide. The white bar represents a distance of 100 nm.

of the L,D,D and D,L,L based gels. The striking features of these images are that the stereochemical differences imposed on the primary structures does not prevent uni-directional self-assembly, with "stacking" of the gelator units still being the dominant motif. In all cases, therefore, highly directional hydrogen bonding formed between amide and carbamate groups on the dendritic peptides appears to persist. However, the stereochemical modification appears to dictate subtle changes in packing behavior. A comparison between organogels composed of D,L,L peptides (Figure 4b) and those composed of L,L,L peptides (Figure 3a) reveals that the D,L,L based gels consist of individual fibres possessing a diameter of about 20 nm. Importantly, the dominant motif of this entangled network was "thick" bundles of individual fibres, typically 200 nm in width, that appeared to be loosely interwoven (relative to the L,L,L based organogel, Figure 3a). A similar comparison can also be drawn between the gel based on D,D,D dendritic peptides (Figure 3g) and the corresponding diastereomer, D,L,L (Figure 4a).

These subtle differences in network morphology may account for the differences observed in the corresponding macroscopic gelation behavior. For example, in the "plateau

region", T_{gel} values for L,D,D and D,L,L based organogels are ca. 50 °C. These values compare to a "plateau region" T_{gel} for L,L,L and D,D,D based gels of ~105 °C. SEM therefore indicates that modifying the stereochemical configuration of the dendritic peptide modulates the packing geometry of the self-assembled state and further evidence for this is provided by small-angle X-ray scattering (SAXS).

Morphological properties of the gel-phase materials--small-angle X-ray scattering (SAXS): Four samples were investigated by SAXS, using the diaminododecane spacer in the presence of two molar equivalents of enantiopure L,L,L, racemic L,L,L/D,D,D, enantiopure L,D,D, and enantiopure D,L,L second-generation dendron. In all cases, X-ray reflections that indicated long-range order were observed (Figure 5).

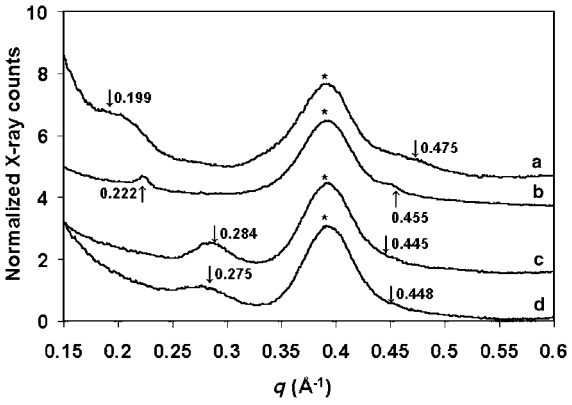

Figure 5. SAXS patterns of gels in toluene using diaminododecane spacer at room temperature with various different dendrons. a) 20 mM L,L,L; b) 10 mM *rac*-L,L,L/D,D,D; c) 20 mM L,D,D; d) 20 mM D,L,L. Arrows highlight peaks identified by peak fit (see also Table 1). Asterisk indicates instrumental artefact.

The patterns of reflections could not be readily interpreted in terms of a common lamellar or hexagonal packing, such as observed in recent studies on 2,3-di-*n*-decyloxyanthracene in propylene carbonate[26] and methyl 4,6-*O*-benzylidene-α-D-mannopyranoside in *p*-xylene.[27] Analysis in terms of packing of hollow cylinders such as performed for organogels of anthraquinone- and azobenzene-appended cholesterol derivatives[28] was not possible as our two-component gel does not have such contrasts in electron densities in its molecular structure.

Although it proved impossible to interpret the data in terms of a specific molecular packing, the observation of diffraction patterns is direct evidence for the order implied in our previous discussions. SAXS indicated (Table 1) that the long range order of the gels constructed using the L,L,L-dendron and the L,L,L/D,D,D racemic mixture are significantly different to one another reflecting their very different morphologies as imaged by SEM. It should also be noted that the patterns of the "mirror-image" gels constructed using either L,D,D or D,L,L have (within error) identical peak positions reflecting the enantiomeric relationship of these materials. Most interestingly, however, the SAXS results provide clear evidence for a significant morphological difference between the L,L,L based gel and the gels based on diastereomeric L,D,D (and D,L,L) peptide—indicating once again that this subtle change in chirality has a clear effect on the assembly process.

Table 1. SAXS peaks and periodicities of gels formed in toluene using various second generation lysine-based dendrons with an N12N (diaminododecane) spacer at 25 °C.

Dendron	Spacer	Peaks
20 mM L, L, L	10 mM N12N	0.199, 0.271, 0.475 $Å^{-1}$ 31.6, 23.2, 13.2 Å
10 mM *rac*-L,L,L/D,D,D	5 mM N12N	0.222, 0.455 $Å^{-1}$ 28.3, 13.8 Å
20 mM L,D,D	10 mM N12N	0.284, 0.445 $Å^{-1}$ 22.1, 14.1 Å
20 mM D,L,L	10 mM N12N	0.275, 0.448 $Å^{-1}$ 22.8, 14.0 Å

Circular dichroism studies: It is well-known that circular dichroism (CD) spectra appear when the chromophoric moieties of chiral molecules are organised into an appropriate orientation.[11,29] The inherent chirality present in the dendritic peptides and the specific orientation of the amide carbonyl groups therefore allowed the three-dimensional structure of the aggregated state to be studied. The investigation was performed at concentrations below the threshold required for macroscopic gelation using cyclohexane as the aprotic solvent. Cyclohexane replaced toluene as the solvent of choice as it exhibits similar physical properties to toluene (and still forms gel-phase materials) but importantly was UV "silent" across the wavelength region of interest (i.e., ~220 nm). Circular dichroism bands were observed for the two-component system, with a λ_{max} value at about 222 nm, ascribable to the amide carbonyl group of the dendritic peptides (Figure 6a). Importantly, no CD signal was observed for the dendritic peptide alone in cyclohexane. This indicates that the CD signals observed for the two-component mixture can be attributed to the helicity of the aggregated state and not to the inherent chirality of the dendritic peptide. It was also confirmed that the contribution of linear dichroism (LD) to the true CD spectra is negligible. This suggests that a chirally organised (probably helical) arrangement is present in the self-assembled state, even below the gelation threshold. Unfortunately, exciton coupling bands that are useful for prediction of the directionality of helicity were not observed.

When a pure L,L,L- or D,D,D-enantiomer based assembled structure (Figure 6a and Figure 6f) was studied, intense equal and opposite CD signals were observed. This indicates that the chiral organisation (helicity) was maximised. It was observed that the helicity of the self-assembled state was related to the enantiomeric purity of the assembly. Reduction of the enantiopurity of the assembly resulted in the loss of helicity, until at a 50:50 racemic mixture the self-assembled state was effectively achiral (Figure 6d). There are three possible explanations for this observation:

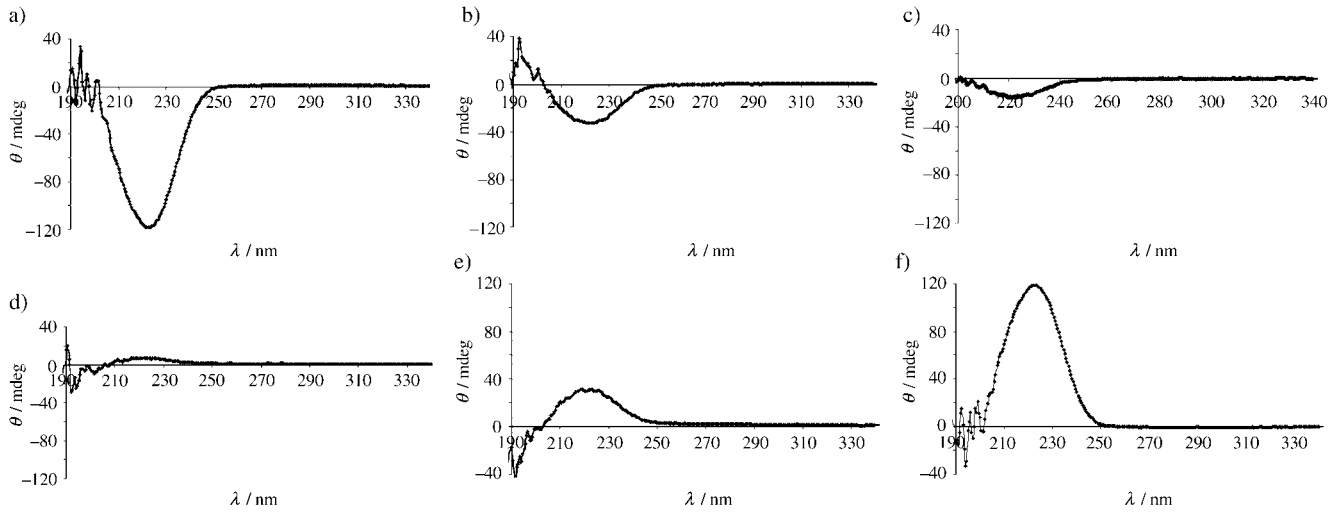

Figure 6. Effect of the stereochemical configuration on the degree of helicity, as indicated by circular dichroism spectra. a) L,L,L(100%):D,D,D(0%); b) L,L,L(75%):D,D,D(25%); c) L,L,L(60%):D,D,D(40%); d) L,L,L(50%):D,D,D(50%); e) L,L,L(25%):D,D,D(75%); f) L,L,L(0%):D,D,D(100%). In each case, [dendritic peptide]$_{total}$ = 3 mM, [$H_2N(CH_2)_{12}NH_2$] = 1.5 mM.

1) The two stereoisomers each form helical fibres with different handedness, the CD effects of which cancel each other out.
2) The two enantiomers attempt to form regions of different handedness on the same fibre, effectively canceling each other out and generating an achiral fibre.
3) The enantiomers disrupt the dominant helicity in a fibre by insertion into the "stack", leading to new nanostructures.

It is worth noting that the loss of helicity is *not* linearly correlated to the incremental addition of the second enantiomer. As shown in Figure 6a–Figure 6c the ellipticity (i.e., the measure of helicity) was reduced from 120 mdeg (Figure 6a) to 30 mdeg (Figure 6b) to 20 mdeg (Figure 6c). These values suggest that the addition of the D,D,D enantiomer to a stereochemically pure L,L,L assembly disproportionately disrupts the helical stacking. Pleasingly, this observation correlates well with the SEM and T_{gel} results and suggests that explanation (3) above is the correct one—as the results clearly contradict explanation (1) and also probably explanation (2). The difference in aggregate morphology observed by SEM between the gel based on the L,L,L stereoisomer (Figure 3a) and the gel based on a mixture L,L,L:[7.5 mM]:D,D,D[2.5 mM] (Figure 3c) is profound. Taken together, these results suggest that the addition of a small amount of the enantiomer not only modifies the level of helicity present in the self-assembled state but also dramatically controls the packing arrangement of the gelator units. As would be expected the gels based on mixtures of enantiomers which are present in inverse ratios provide mirror-image CD spectra - compare for example the CD spectra in Figure 6b [L,L,L(75%):D,D,D(25%)] and Figure 6e [L,L,L(25%):D,D,D(75%)].

The helicity of the self-assembled state was also determined for the L,D,D (Figure 7a) and D,L,L (Figure 7b) dendritic peptides. There is a minimal CD signal in each case (< 10 mdeg), however, the signs of the ellipticities are opposite for each of these compounds reflecting the enantiomeric relationship to one another of the small amount of helicity that is present. This indicates that the supramolecular chiral organisation of these self-assemblies is severely retarded, compared to their L,L,L and D,D,D analogues. Once again, it is very interesting to note that a single chiral centre within a dendritic structure has such a marked effect.

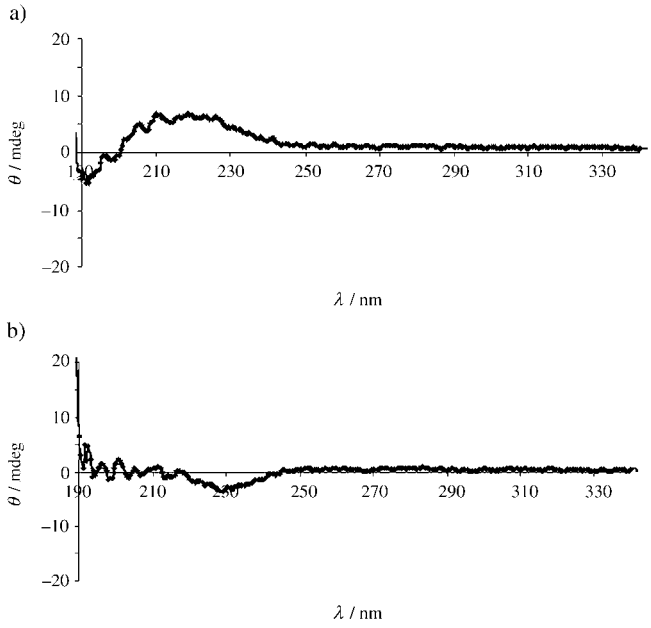

Figure 7. Effect of stereochemical configuration on degree of helicity as shown by circular dichroism spectroscopy a) L,D,D; b) D,L,L. [dendritic peptide]$_{total}$ = 3 mM, [$H_2N(CH_2)_{12}NH_2$] = 1.5 mM.

Intriguingly, SEM indicates that the gelation behavior of the L,D,D and D,L,L based organogels is still based on the microscopic entanglement of fibres, but CD indicates these only possess a minimal degree of helicity. Therefore, we can infer that even though the degree of helicity present in the self-assembly is minimal, a degree of alignment of highly di-

rectional amide-amide hydrogen bonding between gelator units still clearly persists.

Visualisation of chirality on the nanoscale—SEM: From the CD studies, it appears probable that the stereochemistry of the dendritic peptides is expressed on the nanoscale through the formation of fibres that possess inherent helicity. Interestingly, nanoscale helicity was observed for the organogel based on the D,D,D stereoisomer using SEM (Figure 8).

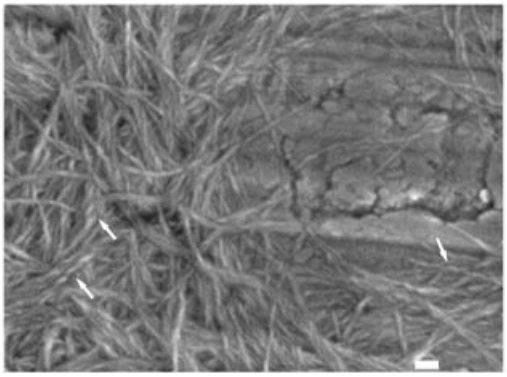

Figure 8. Direct observation of twisting helicity present in a dendritic peptide based organogel, [D,D,D] = 10 mM, [$H_2N(CH_2)_{12}NH_2$] = 5 mM. The white bar represents a distance of 100 nm.

Small regions in which helical intertwining of the fibres was observed were visible (denoted by white arrows). It should be emphasised, that this SEM observation does not necessarily visualise the helicity of a single fibre, but rather may show the helical intertwining of several fibres—a process which could be templated by the inherent helicity of a single fibre. In most cases however, helical twisting could not be determined using SEM, possibly because the sample preparation was too severe.

Conclusion

Aliphatic diamines are solubilised into aprotic solvents by lysine-based dendritic peptides, resulting in optically transparent and thermoreversible gels. The stereochemistry of the lysine groups in the dendritic building blocks plays a key role in controlling the assembly of these soft materials. Notably, the T_{gel} value, which reflects the macroscopic properties of the gel, is dependent on the stereochemistry. Racemic mixtures possess lower T_{gel} values than their single enantiomer analogues. SEM investigations indicate that the racemic gels possess a dramatically different morphology. CD spectrometry indicates the helical nature of the assemblies, and furthermore, indicates that the presence of the "wrong" stereoisomer is able to disrupt the stacking process, breaking-up the well-ordered helical assembly and giving rise to assemblies which have less stereochemical and morphological definition.

Investigation of stereoisomeric gels, in which one chiral centre of the dendritic peptide has been changed, indicates that subtle stereochemical changes can have a profound effect on the self-assembly process. The T_{gel} values of these gels were depressed, SEM indicated a less entangled fibrous network, SAXS indicated a different molecular packing and CD studies implied that the helicity of the fibres being formed was significantly lower. This is a clear example of the impact that chirality can have within a functional dendritic architetcture—a topic which has been of considerable recent interest.[18] Furthermore, the impact of a single structural change on the assembly of fibrillar aggregates is reminiscent of some of the effects observed in biological processes, such as amyloidosis. This indicates the ability of tunable, self-assembling gel-phase materials to act as interesting models for supramolecular disease pathways.

Overall, the results in this paper indicate that for gel-phase materials it is possible to make subtle stereochemical structural modifications which have direct impacts on the nano- and microscale assemblies, as well as on the macroscopic materials properties of the aggregates formed. It is intended that this two-component chiral organogel will potentially provide new chiral self-assembled materials for crystal growth, enantioselective catalysis, separation science and the creation of responsive nanodevices, and investigations in these directions are currently in progress.

Experimental Section

Synthesis and characterisation of dendrons: The four stereoisomeric dendritic peptides were synthesised by using directly analogous methods to that previously reported for L,L,L dendritic lysine,[19] only replacing L-lysine with D-lysine at the appropriate points in the synthesis. Our previous studies have shown that the stereochemistry of these dendritic peptides is retained when employing this synthetic pathway.[20] Purification of these dendritic peptides was achieved using silica gel chromatography. The characterisation of the L,L,L dendritic lysine product was in full agreement with that previously published.[19] IR data and mass spectral data (low and high resolution) were identical for all four dendrons and are therefore not reproduced here. There are distinctive useful differences in the ^{1}H NMR spectra between L,L,L/D,D,D derivatives and their diastereomeric analogues L,D,D/D,L,L. In particular, the N-H protons appear differently, while the CH protons at the chiral centre appear with distinctive chemical shifts dependent on which diastereomer is being studied. It should be noted that all compounds melted across relatively broad ranges (ca. 10 °C), presumably due to a lack of crystallinity—midpoints of the melting ranges are therefore quoted.

L,L,L-dendritic lysine: m.p. 95 °C; $[\alpha]_D^{293}$ −9.3 (c = 1.0, MeOH); ^{1}H NMR (500 MHz, CD_3COCD_3) δ = 7.54 (br s, 1H; CONH), 7.40 (br s, 1H; CONH), 6.17 (d, ^3J = 7.5 Hz, 1H; NHBoc), 6.13 (d, ^3J = 7.5 Hz, 1H; NHBoc), 5.95 (br s, 2H; NHBoc), 4.40 (m, 1H; COC*H*(R)NH), 4.23 (m, 1H;COC*H*(R)NH), 4.07 (m, 1H; COC*H*(R)NH), 3.20–3.10 (br m, 2H; C*H*$_2$NH), 3.06 (m, 4H; C*H*$_2$NH), 1.90–1.30 ppm (54H; m, CH_2 and CH_3).

D,D,D-dendritic lysine: m.p. 95 °C; $[\alpha]_D^{293}$ = +8.9 (c = 1.0, MeOH); ^{1}H NMR identical to L,L,L.

L,D,D-dendritic lysine: m.p. 86 °C; $[\alpha]_D^{293}$ = +9.2 (c = 1.0, MeOH); ^{1}H NMR (500 MHz, CD_3COCD_3) δ = 7.46 (d, ^3J = 7.6 Hz, 1H; CONH), 7.33 (br s, 1H; CONH), 6.13 (s, 1H; NHBoc), 6.00 (s, 2H; NHBoc), ca. 5.7 (v br s, 1H; NHBoc), 4.41 (m, 1H; COC*H*(R)NH), 4.12 (m, 1H; COC*H*(R)NH), 4.04 (m, 1H; COC*H*(R)NH), 3.21 (m, 2H; C*H*$_2$NH), 3.06 (m, 4H; C*H*$_2$NH), 1.90–1.30 ppm (m, 54H; CH_2 and CH_3).

D,L,L-dendritic lysine: m.p. 84 °C; $[\alpha]_D^{293}$ = −14.4 (c = 1.0, MeOH); ^{1}H NMR identical to L,D,D.

Gelation experiments: These experiments were performed by solubilisation of a weighed amount of dendritic gelator in a measured volume of

selected pure solvent. The mixture was sonicated at ambient temperature for 30 min before heating and cooling produced a gel. The gel sample was left to stand overnight. Gelation was considered to have occurred when a homogenous 'solid-like' material was obtained that exhibited no gravitational flow. The thermally reversible gel–sol transition temperature (T_{gel}) was determined by using a tube-inversion methodology.[21]

Scanning electron microscopy: Gel samples were applied to aluminium stubs and allowed to dry. Prior to examination the gels were coated with a thin layer of gold/Pt (60:40). Scanning electron micrographs were recorded by using a Jeol JSM-6330F instrument. Au/Pt deposition was performed using a Denton vacuum LLC.

Small-angle X-ray scattering: SAXS experiments were performed on the SAXS station at the Dutch-Belgian beamline (DUBBLE), BM 26, at the European Synchrotron Radiation Facility in Grenoble, France[30] on organogels mounted in glueless sample cells developed for X-ray absorption spectroscopic studies in organic solvents.[31] SAXS data have been recorded with the gas multi-wire two-dimensional detector at a sample-to-detector distance of 1.4 m, with an X-ray wavelength of 0.93 Å (13.27 eV). The SAXS data were successively normalised for absorption and detector uniformity, and radially averaged. Spatial calibration was reformed with silver behenate[32] with an estimated error margin of $\pm 0.5\%$ in the observed periodicities. The diffraction peaks as well as the background due to solvent scattering and an instrument artifact at $q = 0.4$ Å^{-1} were deconvoluted by using Peakfit v4 (Jandel Scientific).

Circular dichroism measurements: Circular dichroism (CD) spectra were recorded in the ultraviolet region (200–350 nm) using a JASCO 810 spectrometer and a 1.0 mm quartz cuvette. A sample interval of 1 nm and an averaging time of 3 s were used in all experiments. [dendritic branch] = 3 mM.

Acknowledgement

This work was supported by a Leverhulme Trust fellowship (A. R. H.) and The Royal Society (travel grant, ref. 15939). NWO (Dutch Research Council) provided a travel grant and synchrotron radiation facilities at DUBBLE. Dr Igor P. Dolbnya is thanked for support.

[1] a) A. E. Rowan, R. J. M. Nolte, *Angew. Chem.* **1998**, *110*, 65–71; *Angew. Chem. Int. Ed.* **1998**, *37*, 63–68; b) L. J. Prins, D. N. Reinhoudt, P. Timmerman, *Angew. Chem.* **2001**, *113*, 2493–2500; *Angew. Chem. Int. Ed.* **2001**, *40*, 2382–2426; c) D. J. Hill, M. J. Mio, R. J. Prince, T. S. Hughes, J. S. Moore, *Chem. Rev.* **2001**, *101*, 3893–4011; d) D. S. Lawrence, T. Jiang, M. Levett, *Chem. Rev.* **1995**, *95*, 2229–2260; e) J.-M. Lehn, *Angew. Chem.* **1990**, *102*, 1347–1362; *Angew. Chem. Int. Ed. Engl.* **1990**, *29*, 1304–1319.

[2] For general textbooks dealing with supramolecular chemistry see: a) P. D. Beer, P. A. Gale, D. K. Smith, *Supramolecular Chemistry*, Oxford University Press, Oxford, UK, **1999**; b) J. W. Steed, J. L. Atwood, *Supramolecular Chemistry*, Wiley, Chichester, UK, **2000**; for recent articles providing an overview of self-assembly processes see c) G. M. Whitesides, B. Grzybowski, *Science* **2002**, *295*, 2418–2421; d) I. W. Hamley, *Angew. Chem.* **2003**, *115*, 1730–1752; *Angew. Chem. Int. Ed.* **2003**, *42*, 1692–1712.

[3] a) S. Zhang, *Biotechnol. Adv.* **2002**, *20*, 321–339; b) T. Shimizu, *Polym. J.* **2003**, *35*, 1–22; c) M. W. Grinstaff, *Chem. Eur. J.* **2002**, *8*, 2839–2846; d) A. P. Nowak, V. Breedveld, L. Pakstis, B. Ozbas, D. J. Pine, D. Pochan, T. J. Deming, *Nature* **2002**, *417*, 424–428; e) H. A. Klok, J. J. Hwang, J. D. Hartegerink, S. I. Stupp, *Macromolecules* **2002**, *35*, 6101–6111.

[4] a) V. Percec, M. Glodde, T. K. Bera, Y. Miura, I. Shiyanovskaya, K. D. Singer, V. S. K. Balagurusamy, P. A. Heiney, I. Schnell, A. Rapp, H. W. Spiess, S. D. Hudson, H. Duan, *Nature* **2002**, *417*, 384–387; b) J. F. Hulvat, S. I. Stupp, *Angew. Chem.* **2003**, *115*, 802–805; *Angew. Chem. Int. Ed.* **2003**, *42*, 778–781.

[5] For good review articles dealing with organogel assembly see: a) P. Terech, R. G. Weiss, *Chem. Rev.* **1997**, *97*, 3133–3159; b) O. Gronwald, E. Snip, S. Shinkai, *Curr. Opin. Colloid Interface Sci.* **2002**, *7*, 148–156; c) J. H. van Esch, B. L. Feringa, *Angew. Chem.* **2000**, *112*, 2351–2354; *Angew. Chem. Int. Ed.* **2000**, *39*, 2263–2266; d) R. Oda, I. Huc, S. J. Candau, *Angew. Chem.* **1998**, *110*, 2835–2838; *Angew. Chem. Int. Ed.* **1998**, *37*, 2689–2691; e) D. J. Abdallah, R. G. Weiss, *Adv. Mater.* **2000**, *12*, 1237–1247.

[6] For selected papers on the subject of small molecule hydrogelators see: a) Y. Zhang, H. W. Gu, Z. M. Yang, B. Xu, *J. Am. Chem. Soc.* **2003**, *125*, 13680–13681; b) S. Kiyonaka, K. Sugiyasu, S. Shinkai, I. Hamachi, *J. Am. Chem. Soc.* **2002**, *124*, 10954–10955; c) L. A. Estroff, A. D. Hamilton, *Angew. Chem.* **2000**, *112*, 3589–3592; *Angew. Chem. Int. Ed.* **2000**, *39*, 3447–3450.

[7] M. C. Feiters, R. J. M. Nolte, in *Advances in Supramolecular Chemistry, Vol. 6*, (Ed.: G. W. Gokel), JAI Press Inc, Stanford CT, USA, pp. 41–156.

[8] a) M. D. Ward, *Nature* **2003**, *426*, 615–616; b) R. Fasel, M. Parschau, K.-H. Ernst, *Angew. Chem.* **2003**, *115*, 5336–5339; *Angew. Chem. Int. Ed.* **2003**, *42*, 5178–5181.

[9] a) H.-G. Kuball, T. Höfer, in *Chirality in Liquid Crystals* (Eds.: H.-S. Kitzerow, C. Bahr), Springer, New York, **2001**, pp. 67–100; b) R. P. Lemieux, *Acc. Chem. Res.* **2001**, *34*, 845–853.

[10] For a review of supramolecular polymers see: a) L. Brunsveld, J. B. Folmer, E. W. Meijer, R. P. Sijbesma, *Chem. Rev.* **2001**, *101*, 4071–4097; b) J. J. L. M. Cornelissen, A. E. Rowan, R. J. M. Nolte, N. A. J. M. Sommerdijk, *Chem. Rev.* **2001**, *101*, 4039–4070.

[11] See, for example: a) H. Goto, H. Q. Zhang, E. Yashima, *J. Am. Chem. Soc.* **2003**, *125*, 2516–2523; b) J. Makarevic, M. Jokic, Z. Raza, Z. Stefanic, B. Kojic-Prodic, M. Zinic, *Chem. Eur. J.* **2003**, *9*, 5567–5580; c) T. Sumiyoshi, K. Nishimura, M. Nakano, T. Handa, Y. Miwa, K. Tomioka, *J. Am. Chem. Soc.* **2003**, *125*, 12137–12142; d) H. Ihara, T. Sakurai, T. Yamada, T. Hashimoto, M. Takafuji, T. Sagawa, H. Hachisako, *Langmuir* **2002**, *18*, 7120–7123; e) J. J. van Gorp, J. A. J. M. Vekemans, E. W. Meijer, *J. Am. Chem. Soc.* **2002**, *124*, 14759–14769; f) A. Fechtenkötter, N. Tchebotareva, M. Watson, K. Müllen, *Tetrahedron* **2001**, *57*, 3769–3783; g) H. Engelkamp, S. Middelbeek, R. J. M. Nolte, *Science* **1999**, *284*, 785–788; h) S. Tamaru, S. Uchino, M. Takeuchi, M. Ikeda, T. Hatano, S. Shinkai, *Tetrahedron Lett.* **2002**, *43*, 3751–3755; i) J. H. Jung, S. H. Lee, J. S. Yoo, K. Yoshida, T. Shimizu, S. Shinkai, *Chem. Eur. J.* **2003**, *9*, 5307–5313; j) J. H. Jung, H. Kobayashi, M. Masuda, T. Shimizu, S. Shinkai, *J. Am. Chem. Soc.* **2001**, *123*, 8785–8789; k) J. H. Jung, G. John, M. Masuda, K. Yoshida, S. Shinkai, T. Shimizu, *Langmuir* **2001**, *17*, 7229–7232; l) K. Koumoto, T. Yamashita, T. Kimura, R. Luboradzki, S. Shinkai, *Nanotechnology* **2001**, *12*, 25–31; m) U. Maitra, V. K. Potluri, N. M. Sangeetha, P. Babu, A. R. Raju, *Tetrahedron: Asymmetry* **2001**, *12*, 477–480; n) K. Murata, M. Aoki, T. Suzuki, T. Harada, H. Kawabata, T. Komori, F. Ohseto, K. Ueda, S. Shinkai, *J. Am. Chem. Soc.* **1994**, *116*, 6664–6676.

[12] G. M. Whitesides, J. P. Mathias, C. T. Seto, *Science* **1991**, *254*, 1312–1319.

[13] For a review see: D. J. Selkoe, *Nature* **2003**, *426*, 900–904.

[14] D. R. Booth, M. Sunde, V. Bellotti, C. V. Robinson, W. L. Hutchinson, P. E. Fraser, P. N. Hawkins, C. M. Dobson, S. E. Radford, C. C. F. Blake, M. B. Pepys, *Nature* **1997**, *385*, 787–793.

[15] R. Riek, S. Hornemann, G. Wider, M. Billeter, R. Glockshuber, K. Wuthrich, K. *Nature* **1996**, *382*, 180–182.

[16] B. Caughey, P. T. Lansbury, *Annu. Rev. Neurosci.* **2003**, *26*, 267–298.

[17] a) K. S. Partridge, D. K. Smith, G. M. Dykes, P. T. McGrail, *Chem. Commun.* **2001**, 319–320; b) G. M. Dykes, D. K. Smith, *Tetrahedron* **2003**, *59*, 3999–4009; c) A. R. Hirst, D. K. Smith, M. C. Feiters, H. P. M. Geurts, A. C. Wright, *J. Am. Chem. Soc.* **2003**, *125*, 9010–9011; d) A. R. Hirst, D. K. Smith, M. C. Feiters, H. P. M. Geurts, *Langmuir* **2004**, *20*, 7070–7077.

[18] a) B. Romagnoli, W. Hayes, *J. Mater. Chem.* **2002**, *12*, 767–799; b) D. Seebach, P. B. Rheiner, G. Greiveldinger, T. Butz, H. Sellner, *Top. Curr. Chem.* **1998**, *197*, 125–164; c) H. W. I. Peerlings, E. W. Meijer, *Chem. Eur. J.* **1997**, *3*, 1563–1570.

[19] a) R. G. Denkewalter, J. Kolc, W. J. Lukasavage, (Allied Corp) US 4289872, **1981** [*Chem. Abstr.* **1985**, *102*, 79324q]; b) G. M. Dykes, L. J. Brierley, D. K. Smith, P. T. McGrail, G. J. Seeley, *Chem. Eur. J.* **2001**, *7*, 4730–4739.

[20] M. Driffield, D. M. Goodall, D. K. Smith, *Org. Biomol. Chem.* **2003**, *1*, 2612–2620.

[21] a) C. Chaibundit, M. Shao-Min, F. Heatley, C. Booth, *Langmuir* **2000**, *16*, 9645–9652; b) A. Kelarakis, Z. Yang, E. Pousia, S. K. Nixon, C. Price, C. Booth, I. W. Hamley, V. Castelletto, J. Fundin, *Langmuir* **2001**, *17*, 8085–8091.
[22] P. Terech, V. Rodríguez, J. D. Barnes, G. B. McKenna, *Langmuir* **1994**, *10*, 3406–3418.
[23] a) K. Hanabusa, K. Okui, K. Karaki, M. Kimura, H. Shirai, *J. Colloid Interface Sci.* **1997**, *195*, 86–93; b) X. Luo, B. Liu, Y. Liang, *Chem. Commun.* **2001**, 1556–1557;
[24] a) J. H. Fuhrhop, P. Schneider, E. Rosenberg, J. Boekema, *J. Am. Chem. Soc.* **1987**, *109*, 3387–3390; b) J. H. Fuhrhop, W. Helfrich, *Chem. Rev.* **1993**, *93*, 1565–1582.
[25] a) J. Köning, C. Boettcher, H. Winkler, E. Zeitler, Y. Talmon, J. H. Fuhrhop, *J. Am. Chem. Soc.* **1993**, *115*, 693–700; b) C. Boettcher, B. Schade, J. H. Fuhrhop, *Langmuir*, **2001**, *17*, 873–877; c) J. H. Fuhrhop, P. Schnieder, E. Boekema, W. Helfrich, *J. Am. Chem. Soc.* **1988**, *110*, 2861–2867.
[26] M. Lescanne, A. Colin, O. Mondain-Monval, F. Fages, J.-L. Pozzo, *Langmuir* **2003**, *19*, 2013–2020.
[27] K. Sakurai, Y. Jeong, K. Koumoto, A. Friggeri, O. Gronwald, S. Sakurai, S. Okamoto, K. Inoue, S. Shinkai, *Langmuir* **2003**, *19*, 8211–8217.
[28] a) P. Terech, E. Ostuni, R. G. Weiss, *J. Phys. Chem.* **1996**, *100*, 3759–3766; b) K. Sakurai, Y. Ono, J. H. Jung, S. Okamoto, S. Sakurai, S. Shinkai, *J. Chem. Soc. Perkin Trans. 2* **2001**, 108–112.
[29] For examples see: a) E. Snip, S. Shinkai, D. N. Reinhoudt, *Tetrahedron Lett.* **2001**, *42*, 2153–2156; b) H. Ihara, M. Takafuji, T. Sakurai, M. Katsumoto, N. Ushijima, T. Shirosaki, H. Hachisako, *Org. Biomol. Chem.* **2003**, *1*, 3004–3006; c) K. Hanabusa, Y. Maesaka, M. Kimura, H. Shirai, *Tetrahedron Lett.* **1999**, *40*, 2385–2388.
[30] W. Bras, *J. Macromol. Sci. Phys.* **1998**, *37*, 557–565.
[31] V. S. I. Sprakel, M. C. Feiters, R. J. M. Nolte, P. H. F. M. Hombergen, A. Groenen, H. J. R. de Haas, *Rev. Sci. Instrum.* **2002**, *73*, 2994–2998.
[32] T. N. Blanton, T. C. Huang, H. Toraya, C. R. Hubbard, S. B. Robie, D. Louer, H. E. Goebel, G. Will, T. Raftery, *Powder Diffr.* **1995**, *10*, 91–100.

Received: May 20, 2004
Published online: October 7, 2004

